A HIGH-RESOLUTION OBSERVATIONAL AND MODELING COMPARISON OF MESOSCALE BAND LIFE CYCLE DURING THREE RECENT NORTHEAST U.S. SNOWSTORMS

David R. Novak[1,2*], Brian A. Colle[2], and Sandra E. Yuter[3]

[1] NOAA/NWS Eastern Region Headquarters, Scientific Services Division, Bohemia, New York
[2] Stony Brook University, State University of New York, Stony Brook, New York
[3] North Carolina State University, Raleigh, North Carolina

1. INTRODUCTION

Mesoscale band formation on the poleward side of extratropical cyclones can dramatically modify precipitation intensity and accumulation. These bands are especially evident during the cool-season, when their occurrence often results in intense snowfall and extreme snowfall gradients (Kocin and Uccellini 2004, 177–186). Therefore, improving understanding of the structural and dynamical evolution of cool-season mesoscale bands can advance cool-season QPF skill.

Past observational studies have established that bands are often associated with midlevel frontogenesis in the presence of weak moist symmetric stability and sufficient moisture (e.g., Emanuel 1985; Sanders and Bosart 1985; Schultz and Schumacher 1999; Nicosia and Grumm 1999; Novak et al. 2004). Although a basic understanding of the fundamental processes responsible for band formation within the comma-head portion of cyclones has been established, questions remain concerning how changes in forcing, stability, and moisture relate to band life cycle. There is also limited knowledge of the 3D band structure and its evolution.

This study uses single- and dual-Doppler, wind profiler, commercial aircraft, and integrated precipitable water (IPW) vapor observations in concert with model simulations at 4-km grid spacing to investigate the structural and dynamical evolution of three intense banded cases. The three selected banded cases occurred during the 25 December 2002, 12 February 2006, and 14 February 2007 snowstorms. Particular emphasis is placed on common observational and modeling features amongst the banded cases.

2. DATASETS

The relative close proximity of the Binghamton, New York (KBGM) and Albany, New York (KENX) radar sites to each other (165 km) allowed for dual-Doppler synthesis during the 25 December 2002 and 14 February 2007 cases, following the methodology of Yuter and Houze (1995). The WSR-88D polar radar data from KBGM and KENX were interpolated to a common Cartesian grid at 2-km horizontal and 1-km vertical resolution. The wind field was computed within dual-Doppler lobes over eastern New York. Single-Doppler derived wind directions were obtained for the 12 February 2006 case by determining the orientation of the zero isodop at the radial distance corresponding to the desired height (e.g., Wood and Brown 1985). Additional wind observations were obtained for all cases from commercial aircraft (Moninger et al. 2003) and several 915-MHz boundary layer wind profilers. Additionally, ground-based integrated precipitable water (IPW) retrievals (Gutman et al. 2004) near the banded cases were available to verify the simulated moisture fields.

To determine the "best" deterministic simulation for each banded case, a 16-member ensemble was completed using the fifth-generation Penn State/NCAR Mesoscale Model (MM5; Dudhia 1993) and the Weather Research and Forecasting model (WRF; Michalakes et al. 2001). The ensemble was initialized 19-, 18-, and 15-h prior to band formation during the 25 December 2002, 12 February 2006, and 14 February 2007 cases, respectively. Results of this ensemble are reported in Novak et al. (2007). The model configurations of the model forecasts providing the most realistic depiction of the band life cycle in each case are summarized in Table 1. Results from these "best" model forecasts will be presented in this work. The simulations used an outer 36-km domain covering the eastern two-thirds of the U.S. and adjacent coastal waters, and 12-, and 4-km nested (one way) domains centered on the respective banding locations. Thirty-three sigma levels were used in the vertical, with maximum resolution in the boundary layer. The model top was set at 100-hPa. Model terrain was analyzed for the 36-, /12-, and 4-km grids from a 5' and 30" terrain dataset, respectively. A 30" land use dataset from NCAR was used to initialize 25 surface categories for all domains. The 4-km nests were run without convective parameterization. 4-km resolution is expected to be sufficient to resolve the banded frontal circulations, based on previous 2-D idealized modeling by Knight and Hobbs (1988) and Persson and Warner (1993).

Corresponding author address: David Novak, NOAA/NWS Eastern Region Headquarters, 630 Johnson Avenue, Suite 202, Bohemia, NY 11716. Email: david.novak@noaa.gov

Table 1. Model configurations.

Case	Model	Initial/Boundary Conditions	Initialization Time	Convective Scheme	Boundary Layer Scheme	Microphysics Scheme
25 Dec 2002	MM5 (v3.4)	Eta	0000 UTC 25 Dec 2002	Grell	MRF	Simple Ice
12 Feb 2006	MM5 (v3.7)	GFS	1200 UTC 11 Feb 2006	Grell	MRF	Reisner2
14 Feb 2007	MM5 (v3.7)	GFS	0000 UTC 14 Feb 2007	Grell	MRF	Reisner2

3. RESULTS

3.1. Banded case descriptions

The three cyclones exhibited rapid cyclogenesis, with the 25 December 2002 case exhibiting the greatest deepening (25 hPa in 18 h), whereas the 12 February 2006 case exhibited the least (17 hPa in 18 h). All three cases met the criteria of a "bomb", as defined by Sanders and Gyakum (1980). Common features of banded cyclones (e.g., Novak et al. 2004) were present in each case, including the presence of coupled jets, and the development of a closed midlevel circulation (not shown).

Snowfall was extreme in all three cases, with maximum totals of ~100 cm (40 in) during the 25 December and 14 February cases in eastern New York, and a record setting 68.3 cm (26.9 in) in New York City during the 12 February 2006 case. Liquid equivalent precipitation exceeded 40, 70, and 75 mm in the 12 February 2006, 25 December 2002, and 14 February 2006 cases, respectively (Fig. 1). Model forecasts of these cases show an ~35% and 20% under prediction of precipitation in the 25 December 2002 and 12 February 2006 cases, respectively, and an ~15% over prediction in the February 14 2007 case.
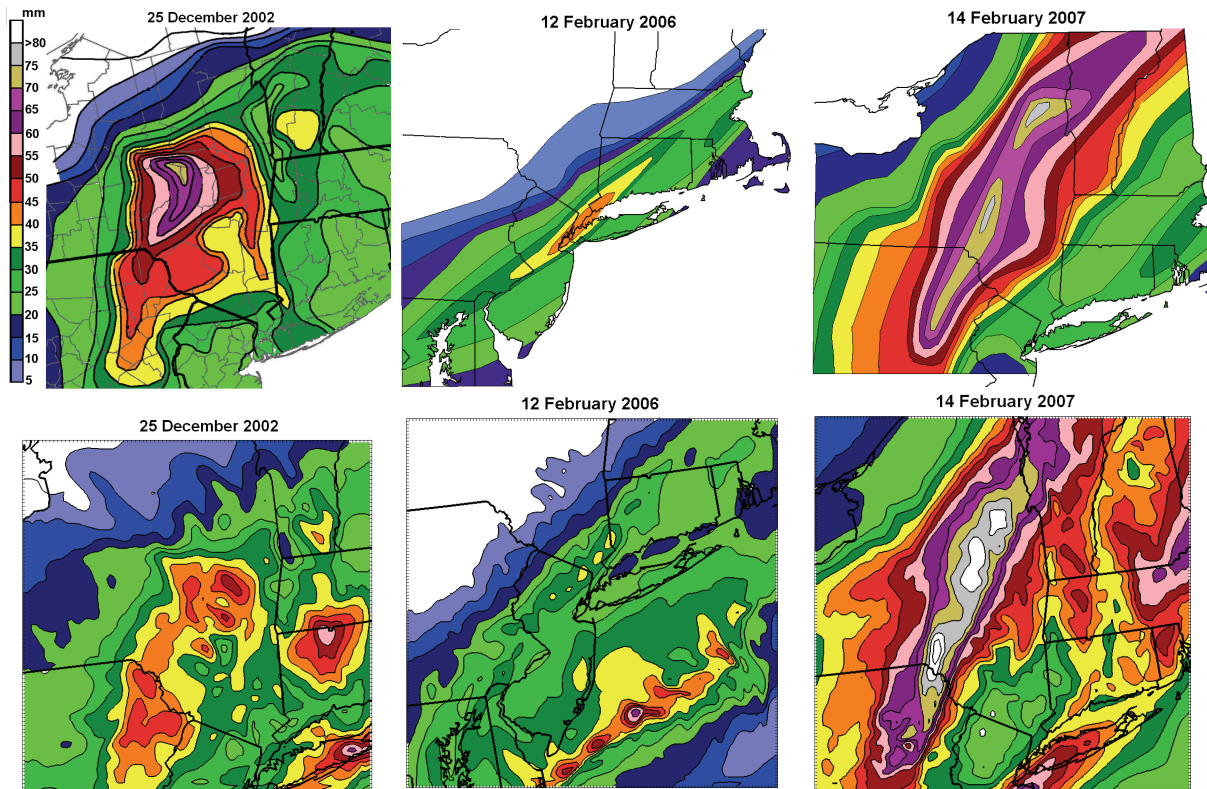

Fig. 1. (top) Manually analyzed cooperative observer storm total liquid equivalent precipitation (mm, shaded every 5 mm according to scale) for the 25 Dec 2002, 12 Feb 2006, and 14 Feb 2007 cases as labeled. (bottom) Corresponding 4-km MM5 model forecast liquid equivalent storm total precipitation.
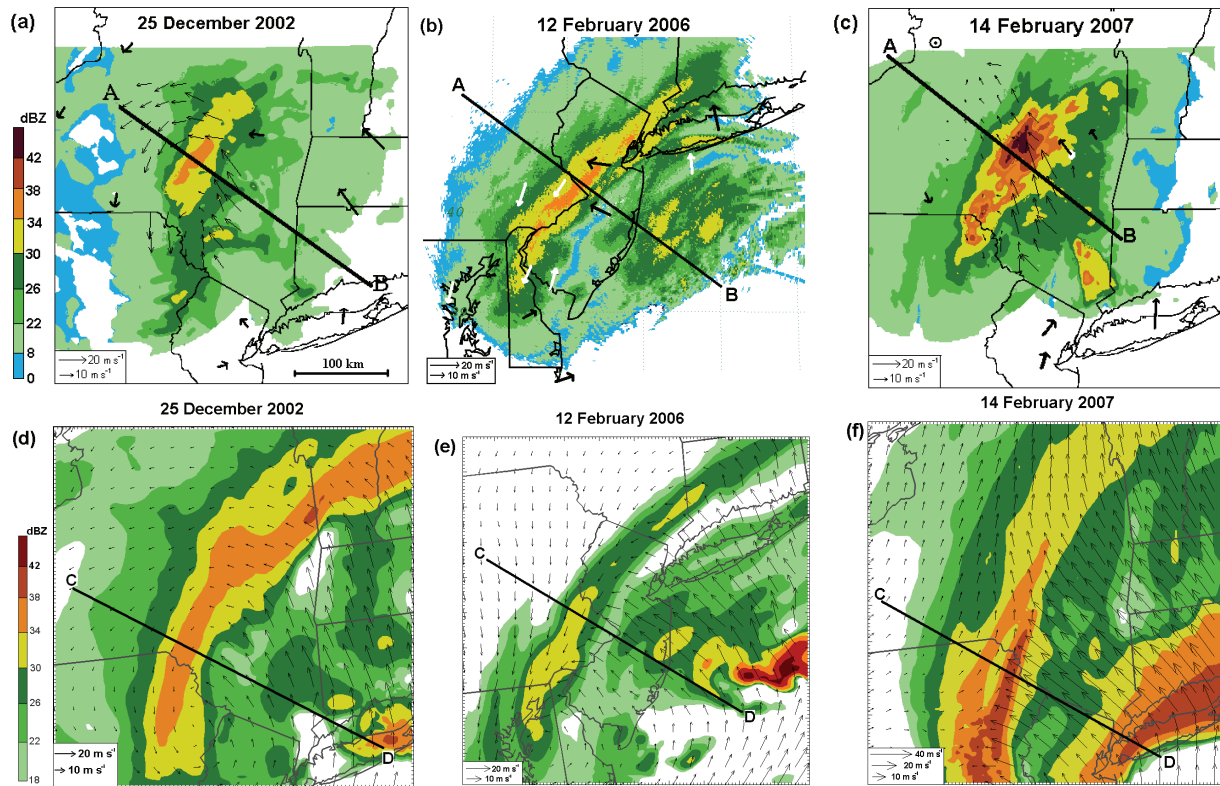
Fig. 2. (a) Observed reflectivity (1-km MSL altitude; shaded according to scale) and 3-km MSL winds (arrows) valid at 1802 UTC 25 Dec 2002. In situ and remote sensing wind observations displayed as thick black arrows. Dual-Doppler winds displayed as this black arrows. (b) As in (a), except valid 1201 UTC 12 Feb 2006. Single-Doppler derived wind direction vectors displayed as white arrows. (c) As in (a), except valid for 1801 UTC 14 Feb 2007. (d–f) Corresponding 4-km MM5 forecast simulated reflectivity (1-km MSL altitude; shaded according to scale) and 3-km MSL wind (arrows).

The analyzed mesoscale evolution of the banded events featured the formation of a midlevel (~3 km MSL) low. This low is evident at the respective times of band maturity in the dual-Doppler, single-Doppler, wind profiler, and aircraft observations over northern New Jersey in the 25 December 2002 case (Fig. 2a), northern Delaware in the 12 February 2006 case (Fig. 2b), and northeast Pennsylvania in the 14 February 2007 case (Fig 2c). A sharp trough extends generally north or northeast from this midlevel low center in each storm. Extreme convergence was found along and to the east of this trough as strong southeast flow slowed, and backed across the trough (Figs. 2a–c).

Corresponding 4-km model simulation fields show the prediction of precipitation bands were within 50 km of the observed location in each case at the time of band maturity (Figs. 2d–f); however, the 12 February 2006 model simulation was time shifted 3 h earlier to obtain the best match. Similar to the observations, a sharp trough was evident in the model wind forecasts (Figs. 2d–f), and was associated with intense frontogenesis (not shown). Frontogenesis in the 14 February 2007 case was particularly extreme with values exceeding 100ºC $(100 \text{ km})^{-1}$ $(h)^{-1}$. These extreme values were a consequence of 60 kt east-southeast wind flow slowing to 10 kt over the span of 30 km (Fig. 2f), in the presence of a 3ºC $(30 \text{ km})^{-1}$ temperature gradient (not shown). The dual-Doppler winds (Fig. 3c) show 50 kt southeast winds. The over prediction of the southeast winds, may have contributed to the overprediction of precipitation in this case.

Cross sections show a sloping region of frontogenesis in each case, with local maxima near the surface in the southeast part of the cross section (near the surface occlusion) and a second maxima near 3 km MSL (Fig. 3). The respective snowbands were associated with this second frontogenesis maxima, with a narrow sloping ascent maximum located above the frontogenesis maxima in the analyses and model forecasts for each case. The ascent maximum was nearly coincident with the frontogenesis maximum, counter to previous theoretical work which predicts the ascent maximum 50–200 km on the warm side of the frontal forcing (e.g., Emanuel 1985; Xu 1992). However, Hakim and Keyser (2001) showed that the value of this displacement is proportional to the static

stability and baroclinicity, and inversely proportional to the inertial stability. In the present case, large inertial stability associated with the sharp cyclonic wind shift was present at the level of maximum frontogenetical forcing (3 km MSL). In this environment of large inertial stability, the ascent maximum is expected to be closer to the frontogenetical forcing.

The cross sections also show that the bands exhibit various tilts (Fig. 3). For example, in the 25 December 2002 case, the observed and modeled cross section shows that the observed reflectivity core sloped downward to the west (Figs. 3a,d). Explicit calculation of hydrometeor trajectories from the model forecast during the 1900–2100 UTC 25 December 2002 period show that this displacement was due to horizontal advection of snow (Fig. 3d), with the band updraft slowing the hydrometeors' fall, and prolonging the time the hydrometeors were subject to horizontal advection in the 600–500-hPa layer.

3.2 Band life cycles

Time series of frontogenesis, ascent, and conditional stability during the life cycle of the modeled bands were constructed in each case to better understand the respective band evolutions. Cross sections from the 4-km model forecasts were examined to determine the magnitude of the midlevel frontogenesis maximum at the base of the band updraft, the 600–400-hPa θ_{es} lapse rate on the equatorward flank of the band updraft, and the magnitude of the ascent within the updraft. A lower tropopause in the 12 February 2006 case relative to the other cases necessitated analyzing stability in the 650–450-hPa layer for this case. The cross section upon which parameters were determined translated with the core of the midlevel frontogenesis maximum with time in each case.
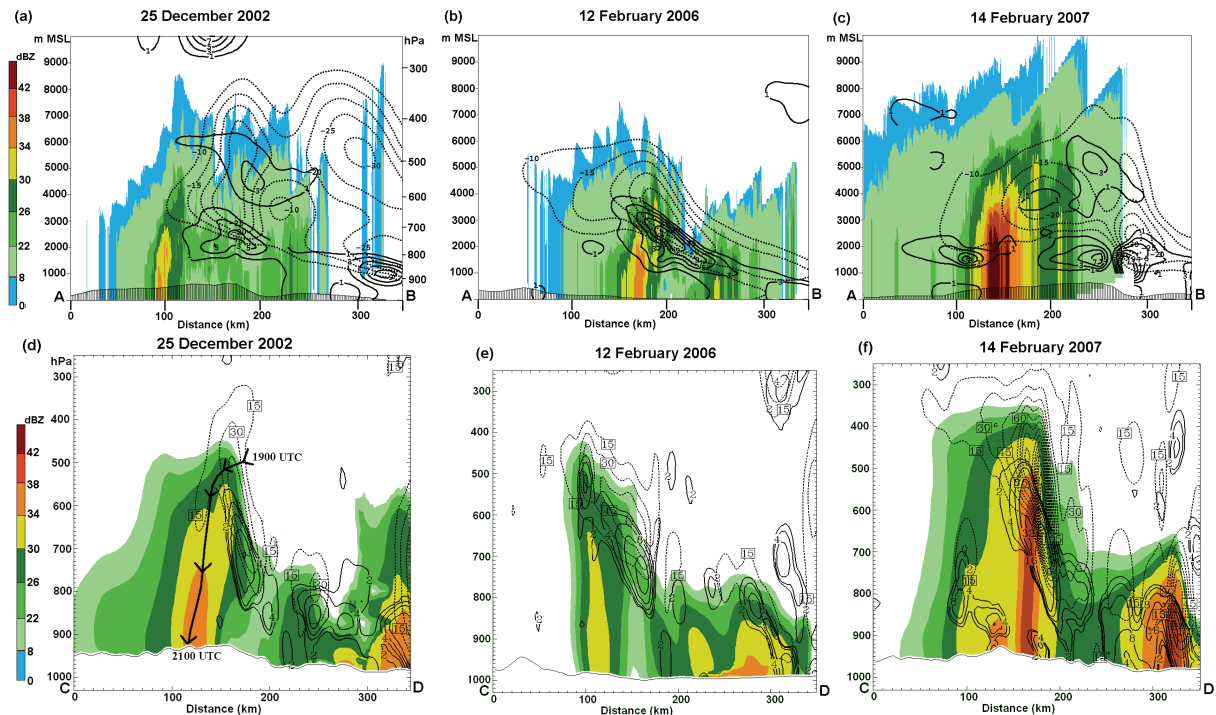

Fig. 3. (a) Radar reflectivity cross section (orientation shown in Fig. 2a) valid at 1802 UTC 25 Dec 2002 with the 1800 UTC Eta analysis Miller 2D frontogenesis [solid, positive values contoured every 2°C (100 km)$^{-1}$ (h)$^{-1}$ starting at 1°C (100 km)$^{-1}$ (h)$^{-1}$], and ascent (dotted, contoured every 5 cm s^{-1} starting at 10 cm s^{-1}). (b) As in (a), except radar reflectivity cross section (orientation shown in Fig. 2b) valid at 1201 UTC 12 Feb 2006 with the 1200 UTC NAM analysis fields overlaid. (c) As in (a), except radar reflectivity cross section (orientation shown in Fig. 2b) valid at 1801 UTC 14 Feb 2007 with the 1800 UTC NAM analysis fields overlaid. (d) 4-km MM5 cross section (orientation shown in Fig. 2d) of model-simulated reflectivity shaded according to scale, Miller 2D frontogenesis [black solid, positive values contoured in multiples of 2°C (100 km)$^{-1}$ (h)$^{-1}$ starting at 2°C (100 km)$^{-1}$ (h)$^{-1}$], and ascent (dotted, contoured every 15 cm s^{-1} starting at 15 cm s^{-1}). The 1900–2100 UTC 25 Dec 2002 hydrometer trajectory in the plane of the cross section is shown by the bold arrows (drawn every 0.5 h). (e) As in (d), except cross section (orientation shown in Fig. 2e) valid 1200 UTC 12 Feb 2006. (f) As in (d), except cross section (orientation shown in Fig. 2f) valid 1800 UTC 14 Feb 2006.

Results show that during the time of band formation, the frontogenetical forcing was increasing, while the layered-averaged conditional stability was small (Fig. 4). Analysis shows there were shallow, embedded layers of conditional instability and inertial instability during the band formation process in each case. The band formed as this instability was released in the sharp convergence zone associated with the developing midlevel trough (e.g., Fig. 2). Ascent exceeding 1 m s^{-1} was forecast during the formation process in each case, with ascent exceeding 2 m s^{-1} in the 14 February 2006 case (Fig. 4), consistent with the heavier precipitation (i.e., Fig. 1).
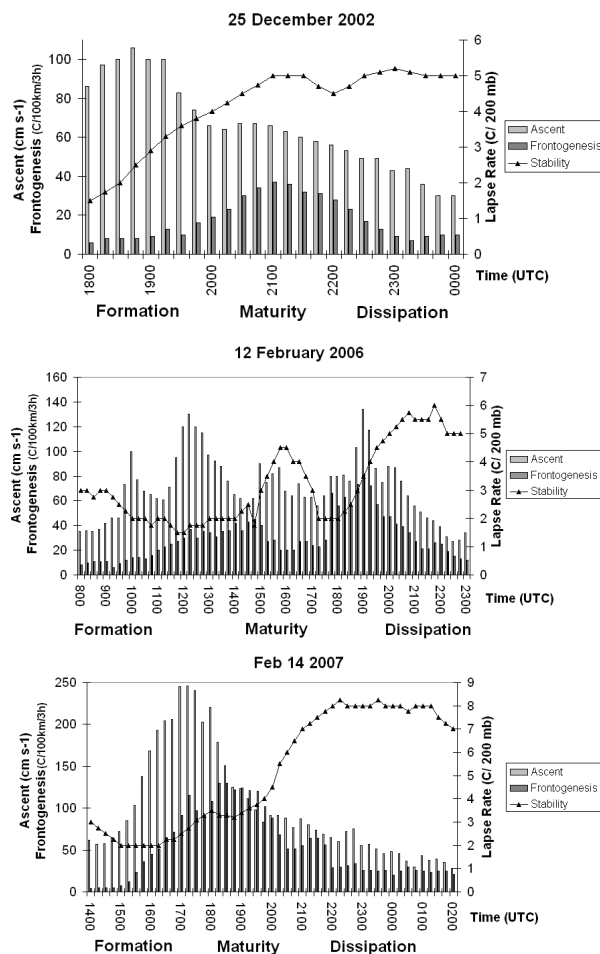

Fig. 4. Time series of midlevel ascent maximum, 2D Miller frontogenesis maximum, and conditional stability in the immediate vicinity of the simulated band for the 25 Dec 2002, 12 Feb 2006, and 14 Feb 2007 cases. See text for details.

During band maturity, the ascent decreased while the stability increased (Fig. 4)— likely a signature of the release of the conditional and inertial instability. The effect of increasing stability was mitigated by increasing frontogenetical forcing, which generally reached a peak during band maturity (Fig. 4). The combined effect was the maintenance of the band. During band dissipation, the midlevel trough weakened, decreasing the frontogenetical forcing. This weaker frontogenesis in the presence of large conditional stability led to band dissipation.

3.3. Model errors

Model errors in the prediction of the band were evident in each case, however, initial investigation has focused on the 25 December 2002 snowstorm, given it exhibited the largest precipitation amount error (~35% underprediction) and a 50 km band position error. Comparisons between high-resolution observations and the model forecasts show that the band position error was tied to an error in the location of the midlevel trough and subsequent location of mesoscale forcing. The early weakening of this trough and associated frontogenesis in the presence of stronger conditional stability than observed led to premature band dissipation in the MM5 forecast (not shown). The greater stability and shorter band duration in the MM5 forecast likely accounted for a majority of the precipitation underprediction, although a small underprediction of integrated precipitatable water vapor in the banded region (not shown) also likely contributed.

4. SUMMARY

Single- and dual-Doppler, wind profiler, aircraft, and IPW observations in concert with MM5 model simulations at 4-km grid spacing were used to conduct a comparison of mesoscale band life cycle during three recent northeast U.S. snowstorms. Results from this study show that the observed and modeled band evolutions were related to changes in forcing, stability, and moisture in each case, validating the importance of these parameters in governing band life cycle.

The observations and model forecasts show band formation was coincident with a pronounced sharpening of a midlevel trough and associated increase in frontogenesis in an environment of conditional and inertial instability. Band dissipation occurred as the midlevel trough became less defined and the frontogenetical flow weakened. The weakening frontogenetical forcing in the presence of conditional stability led to a weakening frontal circulation.

Cross sections through the observed and modeled bands revealed various slopes, which were attributed to hydrometeor advection. Cross sections also revealed that the ascent maximum was found nearly coincident with the frontogenesis maximum counter to previous theoretical work which predicts the ascent maximum 50–200 km on the warm side of the frontal forcing. It was hypothesized very large inertial stability associated with the sharp cyclonic wind shift at the level of maximum frontogenetical forcing (3 km MSL) partially explains this discrepancy.

Future work will focus on determining the governing dynamics of the midlevel trough evolution within a potential vorticity framework. The potential vorticity framework will also be used to diagnose model errors associated with each case.

5. ACKNOWLEDGMENTS

6. REFERENCES

Dudhia, J., 1993: A nonhydrostatic version of the Penn State–NCAR mesoscale model: Validation tests and simulation of an Atlantic cyclone and cold front. *Mon. Wea. Rev*., **121**, 1493–1513.

Emanuel, K. A., 1985: Frontal circulations in the presence of small moist symmetric stability. *J. Atmos. Sci*., **42**, 1062–1071.

Gutman, S. I., S. R. Sahm, S. G. Benjamin, B. E. Schwartz, K. L. Holub, J. Q. Stewart, and T. L. Smith, 2004: Rapid retrieval and assimilation of ground based GPS precipitable water observations at the NOAA Forecast Systems Laboratory: Impact on weather forecasts. *J. Meteor. Soc. of Japan*, **82**, 1–10.

Hakim, G. J., and D. Keyser, 2001: Canonical frontal circulation patterns in terms of Green's functions for the Sawyer–Eliassen equation. *Quart. J. Roy. Meteor. Soc.*, **127**, 1795–1814.

Knight, D. J., and P. V. Hobbs, 1988: The mesoscale and microscale structure and organization of clouds and precipitation in mid-latitude cyclones. Part XV: A numerical modeling study of frontogenesis and cold-frontal rainbands. *J. Atmos. Sci.*, **45**, 915–930.

Kocin, P. J., and L. W. Uccellini: Northeast Snowstorms. Volume 1: Overview. Meteor. Monogr., No. 54, Amer. Meteor. Soc., 296 pp.

Michalakes, J., S. Chen, J. Dudhia, L. Hart, J. Klemp, J. Middlecoff, and W. Skamarock, 2001: Development of a next generation regional weather research and forecast model. *Developments in Teracomputing: Proceedings of the Ninth ECMWF Workshop on the Use of High Performance Computing in Meteorology,* W. Zwieflhofer and N. Kreitz, Eds., World Scientific, Singapore, 269–276.

Moninger, W. R., R. D. Mamrosh, and P. M. Pauley, 2003: Automated meteorological reports from commercial aircraft. *Bull. Amer. Meteor. Soc*., **84**, 203–216.

Nicosia, D. J., and R. H. Grumm, 1999: Mesoscale band formation in three major northeastern United States snowstorms. *Wea. Forecasting*, **14**, 346–368.

Novak, D. R., L. F. Bosart, D. Keyser, and J. S. Waldstreicher, 2004: An observational study of cold season-banded precipitation in northeast U.S. cyclones. *Wea. Forecasting*, **19**, 993–1010.

——, and B. A. Colle, 2007: Assessing Predictability of Band Formation and Evolution during Three Recent Northeast U.S. Snowstorms. Preprints, *22th Conference on Weather Analysis and Forecasting/18th Conference on Numerical Weather Prediction*, Park City, UT, Amer. Meteor. Soc., P1.29A.

Persson, P. O. G., and T. T. Warner, 1993: Nonlinear hydrostatic conditional symmetric instability: Implications for numerical weather prediction. *Mon. Wea. Rev.*, **121**, 1821–1833.

Sanders, F., and J. R. Gyakum, 1980: Synoptic-dynamic climatology of the "bomb". *Mon. Wea. Rev.*, **108**, 1589–1606.

——,and L. F. Bosart, 1985: Mesoscale structure in the megalopolitan snowstorm of 11–12 February 1983. Part I: Frontogenetical forcing and symmetric instability. *J. Atmos. Sci*., **42**, 1050–1061.

Schultz, D. M., and P. N. Schumacher, 1999: The use and misuse of conditional symmetric instability. *Mon. Wea. Rev*., **127**, 2709–2732; Corrigendum, **128**, 1573.

Wood, V. T., and R. A. Brown, 1985: Single Doppler velocity signature interpretation of nondivergent environmental winds. *J. Atmos. Ocean. Tech*., **3**, 114–128.

Xu, Q., 1992: Formation and evolution of frontal rainbands and geostrophic potential vorticity anomalies. *J. Atmos. Sci*., **49**, 629–648.

Yuter, S. E., and Houze, R. A. Jr., 1995: Three-Dimensional kinematic and microphysical evolution of Florida cumulonimbus. Part I: Spatial distribution of updrafts, downdrafts, and precipitation. *Mon. Wea. Rev*., **123**, 1921–1940.